2-Arylidene Hydrazinecarbodithioates as Potent, Selective Inhibitors of Cystathionine γ-Lyase (CSE)

Abir Bhattacharjee,[†] Antara Sinha,[†] Kiira Ratia, [#]
Liang Yin, [#] Loruhama Delgado-Rivera,[#] Pavel A. Petukhov,[#] Gregory R. J. Thatcher,[#] and Duncan J. Wardrop*[†]

[†]Department of Chemistry, University of Illinois at Chicago, 845 W. Taylor St., Chicago, Illinois 60607, United States

[#]Department of Medicinal Chemistry & Pharmacognosy, University of Illinois College of Pharmacy, University of Illinois at Chicago, 833 S. Wood St., Chicago, IL 60612, United States

Supporting Information, Part 1

Table of Contents

1. GENERAL COMMENTS

Expression and purification of full-length, recombinant human CSE and CBS enzymes was performed according to published protocols,[1,2] with the exception of using His-tag as opposed to using the GST plasmid described in these methods. AzMC was purchased from Sigma-Aldrich and CPM was purchased from Molecular Probes. Enzymatic assays were assembled in 384-well plates on a Tecan Freedom EVO liquid handling workstation equipped with a plate shaker, and compounds were delivered to assay wells by 384-pin devices (V&P Scientific). Assay fluorescence was measured on a Tecan Infinite F200 Pro equipped with appropriate filters.

All non-aqueous reactions were carried out in oven- or flame-dried glassware under an atmosphere of nitrogen, unless otherwise noted. All solvents were reagent grade. Triethylamine was distilled from calcium hydride, under nitrogen, and stored over potassium hydroxide. *N,N*-Dimethylformamide (DMF) was purchased from a commercial vendor and dried with freshly activated 4 Å molecular sieves prior to use. All products were purified by flash column chromatography using silica gel 60 (mesh 230-400) either manually, or using a CombiFlash Rf+ chromatography system unless otherwise noted. All other reagents and starting materials were purchased from commercial vendors and used without further purification. All melting points were determined in open Pyrex capillaries with a Thomas Hoover Unimelt melting point apparatus and are uncorrected. ^{1}H and ^{13}C spectra were recorded on a Bruker Avance 400 (400 MHz ^{1}H, 100 MHz ^{13}C) or a Bruker Avance 500 (500 MHz ^{1}H, 125 MHz ^{13}C) spectrometer. The purity of all compounds assayed was determined by analytical HPLC using a Shimadzu HPLC (dual wavelength, $\lambda = 270$ nm) and a 25 x 4 mm, 5 micron C_{18} Keystone Scientific column. Gradient solvent consisted of 0.1% TFA and 0-100% acetonitrile in water over 20 minutes and thereafter 100% acetonitrile maintaining a constant flow rate of 1.5 ml/min.

2. HIGH-THROUGHPUT SCREENING FOR CSE INHIBITORS

High-throughput screening of human CSE against >100,000 compounds was performed using a fluorescence-based primary assay. The assay directly monitors the formation of cysteine, a product of cystathionine cleavage, using a thiol-reactive, fluorogenic reagent (7-diethylamino-3-(4'-maleimidylphenyl)-4-methylcoumarin (CPM)). HTS with the primary assay was performed in duplicate at room temperature in black 384-well plates, and all test wells (50 μL) contained the following reagents: 100 mM purified CSE, 100 μM L-cystathionine, 20 μM PLP, 50 mM Tris pH 8.5, 0.1 mg/mL bovine serum albumin (BSA), 0.01% Triton-X 100, 50 μM CPM, and 40 μM test compound. Enzymatic reactions were monitored continuously for 7 minutes (excitation: 400 nm, emission: 535 nm), and slopes were recorded of the linear portion of the progress curve. All assay plates contained 32 positive control wells (10 μM L-PAG), 32 negative control wells (DMSO), and 320 test wells (40 μM compound). Z'-factors per plate, which were calculated from control wells to assess assay quality over the course of the screen, were consistently greater than 0.7, indicating a robust, high quality screen.[3]

3. HIT VALIDATION

The CSE H_2S assay contained 50 mM Tris pH 8.5, 500 nM CSE, 2.5 mM L-cysteine, 20 μM PLP, and 120 nM azido-methylcoumarin (AzMC).[4] The CBS H_2S assay contained 50 mM Tris pH 8.5, 80 nM recombinant human CBS, 2.5 mM L-cysteine, 2.5 mM L-homocysteine, 240 μM S-adenosylmethionine, 20 μM PLP, and 120 μM AzMC. Reactions (50 μL) were carried out in black 384-well plates at 37°C. Conversion of AzMC to 7-amino-4-methylcoumarin by H_2S was monitored continuously for 45 min (excitation: 360 nm, emission: 460 nm). Slopes of the linear portion of the progress curve were recorded for each well and normalized to plate-based controls.

4. DETERMINATION OF THE IC_{50} VALUES OF INHIBITORS

The IC_{50} values of all tested inhibitors were measured using the primary screen CPM assay described above. Briefly, following a 15-minute pre-incubation of enzyme with various concentrations of compound (100, 50, 25, 12.5, 6.25, 3.13, 1.56, and 0.78 μM) at room temperature, the enzymatic reaction was initiated by addition of L-cystathionine and CPM. Plates were shaken vigorously for 30s, and fluorescence was detected continuously for 7 minutes. Slopes of the progress curves were recorded and percent enzyme inhibition was calculated using the following equation: $\%I = [1-(slope_{sample} - slope_{blank})/(slope_{control} - slope_{blank})] \times 100$ where $slope_{control}$ is the average slope of 16 wells of DMSO-treated CSE, representing 0% inhibition, and $slope_{blank}$ is the average of 16 wells of assay mix lacking CSE, representing 100% inhibition. IC_{50} values were calculated by plotting %I against inhibitor concentration and fitting the data in Prism 7 (GraphPad Software).

5. REVERSIBILITY OF INHIBITORS

To test inhibitor reversibility, 1 mL of 120 nM CSE enzyme was incubated with 50 μM inhibitor for 2 h at room temperature in Buffer A (50 Tris pH 8.5 and 5 μM PLP). Enzyme inactivation was confirmed by testing an aliquot in the CPM assay. 500 μL of the above sample was placed in a Slide-A-Lyzer mini dialysis device (10K MWCO) and dialyzed against 15 mL of Buffer A with gently shaking at room temperature, with 3 buffer changes occurring over 24 h. Undialyzed samples were incubated alongside dialyzed samples. Following 18, 24, 48 h, the dialyzed and undialyzed samples were tested in the CPM activity to assess the reversibility of

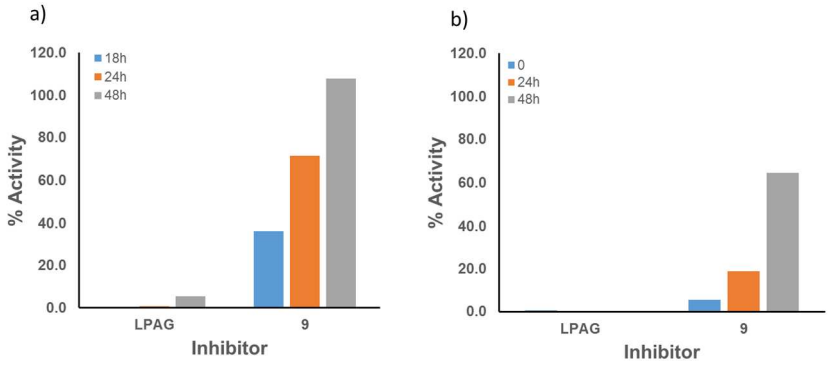

Figure S1. Activity assay of a) dialyzed samples of CSE treated with L-PAG and 9, looking at 18, 24 and 48 h; b) undialyzed samples at 0, 24 and 48 h.

enzyme inactivation (**Figure S1**).

6. MOLECULAR MODELLING STUDIES

Coordinates of X-ray model of CSE 2NMP and 3COG[1] were downloaded from the protein data bank (PDB). Docking studies were performed in Molecular Operating Environment (MOE).[5] The proteins were subjected to the "structure preparation" procedure. Hydrogen atoms were added using the Protonate3D algorithm. The energy of the resulting structure was minimized with AMBER12EHT forcefield[6,7] until gradient RMS was less than 0.001 kcal/mol/Å^2. The CSE inhibitors were assigned MMFF94x charges and minimized using the

MMFF94x forcefield until the RMS gradient was less than 0.001 kcal/mol/Å.[2] The MOE docking module "Dock" was used for docking/scoring using the default parameters and settings. PLP and L-PAG were used to define the binding site. Docking was performed using the "induced fit" algorithms, "Triangle Matcher" for placement, "London dG" for scoring of the binding poses after placement, and "GBVI/WSA dG" for rescoring of the resulting poses. For analysis of the interactions and the figure shown in the main manuscript, docked ligand **43** and CSE were additionally co-minimized using the same parameters as those specified above. The details of the protein-ligand interactions are shown in **Figure S2**.

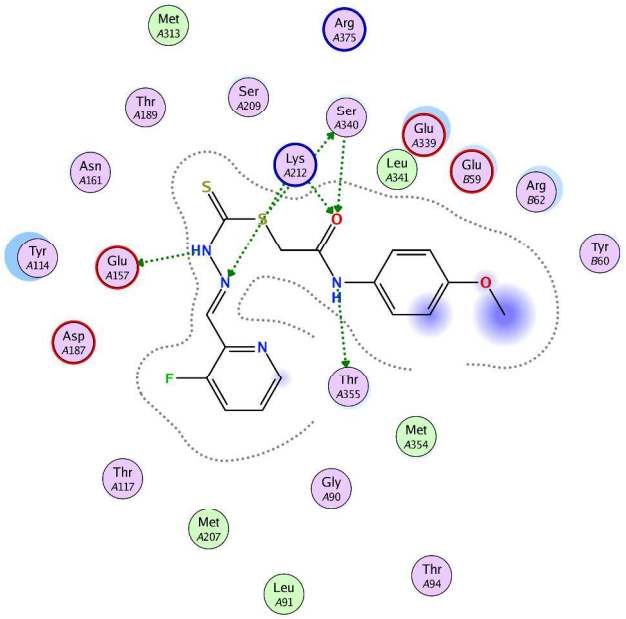

Figure S2. Protein-ligand interaction between CSE (PDB: 2NMP) and ligand **43**. The 2D depiction of protein-ligand interactions is described in ref. 7

Upon inspection of the binding site, we noted that **43** and other ligands in this series were too large to fit the binding site containing PLP. The limited space available to the inhibitors in the

presence of PLP and similarity between **43** and the intermediates formed between cystathionine and PLP suggested that 2-arylidene hydrazinecarbodithioates may mimic their binding pose and, hence, all the docking studies were conducted without PLP. A representative example of **43** docked to CSE is shown in **Figure S2** and **Figure S3**.

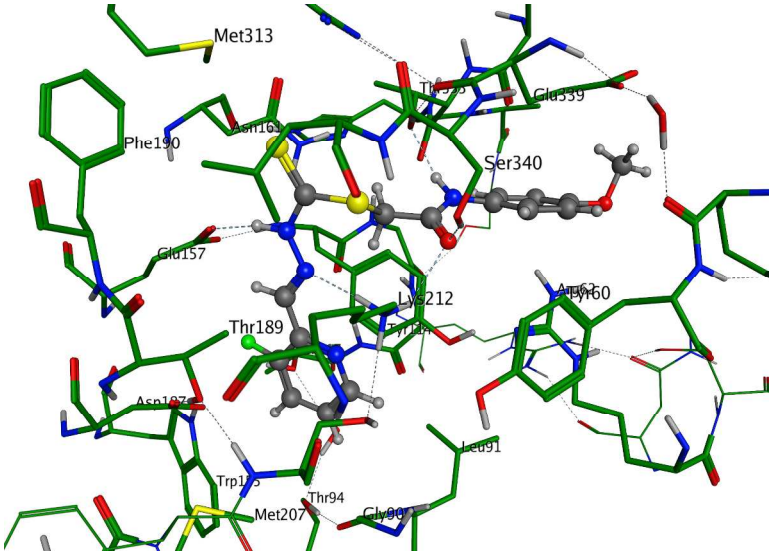

Figure S3. Inhibitor **43** Docked to Cystathionine γ-Lyase (CSE).

The docked poses of all the other compounds in this series are analogous to that of **43**. The 6-fluoro-2-pyridyl group of **43** occupies approximately the same location as the pyridyl group of PLP in the pocket formed by Tyr114, Thr117, Trp155, Met207, Gly90, Asp187, Thr189, and Ser209. Similarly to PLP, it forms hydrophobic face-to-face π-π interaction with Tyr114. If Lys212 is protonated, it can potentially form strong coulombic interactions/salt bridge with the pyridyl nitrogen as the distance between them is only 2.9 Å. The SAR suggests that contribution of this charge-charge interaction is important because changes in the position of the nitrogen in the ring and a substituent in the proximity of the 2-pyridyl nitrogen result in a decrease in potency. The lone pair of the sp^2 nitrogen and NH group in the hydrazone moiety of **43** form

hydrogen bonds with Lys212 and Glu175, respectively. The thioester group of **43** occupies the hydrophobic pocket formed by Met313, Phe190, Leu341, Thr355, and the hydrophobic portion of the sidechain of Asn161. The amide bond of **43** participates in extensive network of hydrogen bonds with Lys212, Ser340, and Thr355. The gorge region of the binding site, which is occupied by L-PAG in the X-ray model 3COG, accommodates the 4-methoxyphenyl group of **43**, with the OCH_3 moiety pointing toward the solvent. The hydrophobic portions of the side chains of Glu339, Tyr114, and Tyr60 form a tight pocket suitable for a substituent as large as phenyl group. In this pocket, the substituents can only be placed in the para position of the phenyl ring in R_2 in ligands **31**-**55** as otherwise they would clash with the narrow gorge region on the binding site. The ability of the binding site to accommodate linear aryl substituents is supported by the SAR. Not only **36** with a *m*-bromophenyl substituent lost its activity against CSE completely but also compounds **31**-**55** are on average more potent than compounds **8**, **17**-**30**, which lack the aryl substituent. Additionally, Arg62 appears to be sufficiently close (c.a. 3.3 Å) to the 4-methoxyphenyl group of **43** to form a cation-π interaction. This placement of the aryl substituent in **31**-**55** is also indirectly supported by the SAR since compounds with electron-donating methyl, *t*-butyl, and especially OCH_3 groups were generally more potent than the corresponding analogs **35** and **44** with electron-withdrawing fluoro and CF_3 substituents, respectively.

7. GENERAL PROCEDURES SYNTHETIC PROCEDURES

7.1. General Procedure A (Preparation of (*E*)-2-Arylidene hydrazinecarbodithioates)

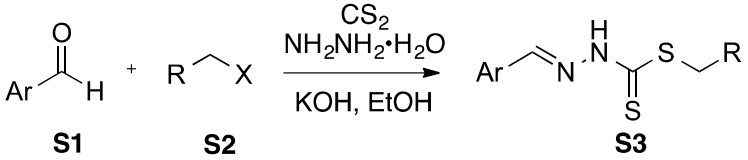

To a solution of hydrazine monohydrate (1.1 equiv, 55 %) in absolute EtOH (0.2 M) at 0 °C was added powdered KOH (1.1 equiv), carbon disulfide (1.1 equiv) and alkyl halide (1.1 equiv).

The resulting mixture was stirred at room temperature for 1-3 h and the corresponding aldehyde (1.0 equiv) was added. The reaction mixture was stirred for a further 3 h at room temperature, concentrated under reduced pressure and filtered. The precipitate was washed with water and the crude product obtained was further purified by flash column chromatography to provide the desired products in 60-80% yields.

7.2. General Procedure B (Preparation of Aryl hydrazones)

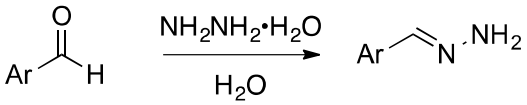

S1 **S4**

A mixture of aldehyde (1 equiv) and hydrazine hydrate (7 equiv) solution, 55% in water, was heated at 90 ºC for 2 h. The solution was cooled and partitioned between CH_2Cl_2 (2 mL/mol) and water (1 mL/mol) and the phases separated. The aqueous phase was extracted CH_2Cl_2 (x3, 2 mL/mol). The combined organic extracted were dried over $MgSO_4$, filtered and the filtrate concentrated under reduced pressure to provide the hydrazone, which was used in the subsequent step without further purification.

7.3. General Procedure C (Preparation of 5-Aryl-1,3,4-thiadiazolidine-2-thiones)

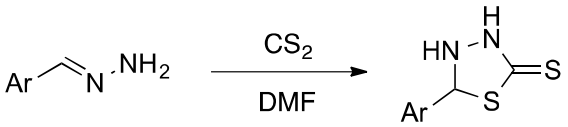

S4 **S5**

A solution of hydrazone (1 equiv) and carbon disulfide (7 equiv) in DMF (0.2 mL/mmol) was heated at reflux for 6 h. After cooling to room temperature, the reaction mixture was concentrated under reduced pressure and poured into ice-cold water. After settling for 1 h, the resulting precipitate was filtered off, washed with water and then dried under reduced pressure. This product was used in the subsequent step without further purification.

7.4. General Procedure D (Preparation of (*E*)-2-Arylidene hydrazinecarbodithioates)

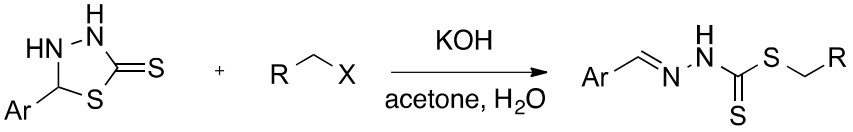

S5 **S2** **S3**

A mixture of thiadiazolidine-2-thione (1 equiv) and powdered KOH (1 equiv) in acetone (2 mL/mmol) and water (2 mL/mmol) was stirred until all solids dissolved. A solution of alkyl halide (1 equiv) in acetone (2 mL/mmol) was added to the reaction mixture stirred at room temperature for 1 h, during which time a yellow solid precipitated. This material was removed by filtration, washed with cold EtOH, dried and then purified by flash column chromatography to provide the desired products 60-80% yield.

8. EXPERIMENT DETAILS

8.1. Methyl (*E*)-2-(pyridin-2-ylmethylene)hydrazine-1-carbodithioate (8)

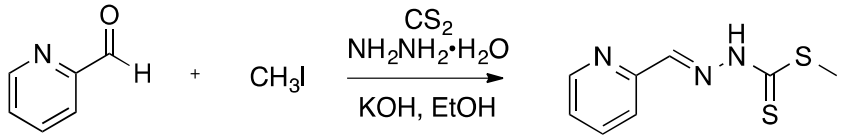

S6 **S7** **8**

Following Procedure A, picolinaldehyde (1.00 g, 9.33 mmol) was converted to compound **8** (1.49 g, 7.09 mmol, 76%), a yellow solid (mp 170-172 °C decomp); t_R-HPLC: 17.3 min (96%); ^{1}H NMR (500 MHz, DMSO-d6) δ 8.64-8.60 (m, 1H), 8.27 (s, 1H), 7.94-7.86 (m, 2H), 7.46-7.42 (m, 1H), 3.34 (s, 1H), 2.54 (s, 3H); ^{13}C NMR (125 MHz, DMSO-d6) δ 199.36, 152.34, 149.80, 146.43, 137.01, 124.88, 120.01, 16.85; FTIR υ_{max} 3088, 3002, 2914, 2795, 1597, 1529, 1466, 1435, 1419, 1311, 1280, 1263, 1146, 1106, 1080, 1040, 999, 955, 927, 876, 863, 776, 744, 726, 680, 633, 597, 578 cm^{-1}; ESI-MS (m/z) calcd for $C_8H_9N_3S_2$ $[M+H]^+$ 212.0316, found: 212.0309.

8.2. Methyl (*E*)-2-(pyridin-3-ylmethylene)hydrazine-1-carbodithioate (17)

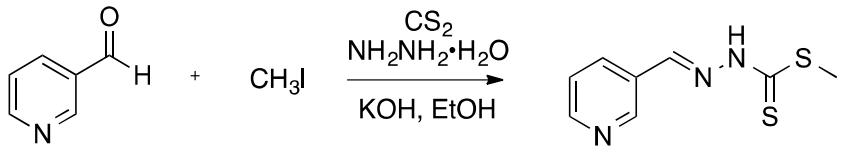

S8 **S7** **17**

Following Procedure A, nicotinaldehyde (0.70 g, 6.53 mmol) was converted to compound **10** (1.00 g, 4.77 mmol, 73%), a yellow solid (mp 170-172 °C decomp); t_R-HPLC: 17.3 min (98%); ^{1}H NMR (500 MHz, DMSO-d6) δ 8.86 (d, *J* = 1.65 Hz, 1H), 8.64 (dd, *J* = 1.5, 4.7 Hz, 1H), 8.28 (s, 1H), 8.13 – 8.09 (m, 1H), 7.50 (dd, *J* = 4.9, 7.9 Hz, 1H), 2.53 (s, 3H); ^{13}C NMR (125 MHz, DMSO-d6) δ 198.96, 151.21, 148.99, 143.60, 133.73, 129.46, 124.12, 16.80; FTIR υ_{max} 3111, 3036, 2987, 2917, 1604, 1540, 1427, 1354, 1316, 1297, 1241, 1192, 1125, 1107, 1050, 1038,

957, 929, 906, 871, 799, 732, 698, 675, 632, 606, 596 cm^{-1}; ESI-MS (m/z) calcd for $C_8H_{10}N_3S_2$ $[M+H]^+$ 212.0316, found: 212.0316.

8.3. Methyl (*E*)-2-(pyridin-4-ylmethylene)hydrazine-1-carbodithioate (18)

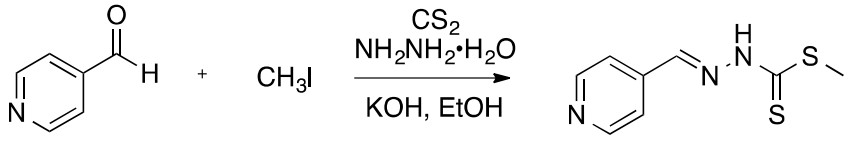

S9 **S7** **18**

Following Procedure A, isonicotinaldehyde (0.50 g, 4.67 mmol) was converted to compound **12** (0.74 g, 3.50 mmol, 75%), a yellow solid (mp 169-171 °C decomp); t_R-HPLC: 17.3 min (98%); ^{1}H NMR (500 MHz, DMSO-d6) δ 8.66 (d, *J* = 6.0 Hz, 2H), 8.22 (s, 1H), 7.65 (d, *J* = 6.0 Hz, 2H), 2.54 (s, 3H); ^{13}C NMR (125 MHz, DMSO-d6) δ 199.78, 150.411, 143.70, 140.60, 121.08, 16.85; FTIR υ_{max} 3074, 2955, 2916, 1594, 1556, 1416, 1357, 1329, 1283, 1227, 1204, 1106, 1082, 1040, 999, 958, 914, 875, 801, 731, 668, 599 cm^{-1}; ESI-MS (m/z) calcd for $C_8H_{10}N_3S_2$ $[M+H]^+$ 212.0316, found: 212.0323.

8.4. Methyl (*E*)-2-(1-(pyrdin-2-yl)ethylidene)hydrazine-1-carbodithioate (19)

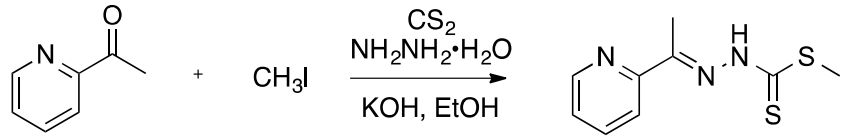

S10 **S7** **19**

Following Procedure A, 1-(pyridin-2-yl)ethan-1-one (0.20 g, 1.65 mmol) was was converted to compound **14** (0.24 g, 1.09 mmol, 66%), a yellow solid (mp 172-174 °C decomp); t_R-HPLC: 17.3 min (96%); ^{1}H NMR (400 MHz, DMSO-d6) δ 8.65 – 8.61 (m, 1H), 8.11 – 8.07 (m, 1H), 7.91 – 7.85 (m, 1H), 7.48 – 7.43 (m, 1H), 2.53 (s, 3H), 2.46 (s, 3H); ^{13}C NMR (100 MHz, DMSO-d6) δ 200.75, 154.32, 151.75, 148.87, 136.80, 124.60, 120.35, 17.09, 17.95; FTIR υ_{max} 3146, 3067, 2987, 2913, 1578, 1562, 1483, 1460, 1428, 1366, 1336, 1244, 1144, 1114, 1085, 1060, 1044, 991, 949, 886, 774, 734, 679, 643, 621, 579, 562 cm^{-1}; ESI-MS (m/z) calcd for $C_9H_{12}N_3S_2$ $[M+H]^+$ 226.0473, found: 226.0470.

8.5. Methyl (*E*)-2-(pyrazin-2-ylmethylene)hydrazine-1-carbodithioate (20)

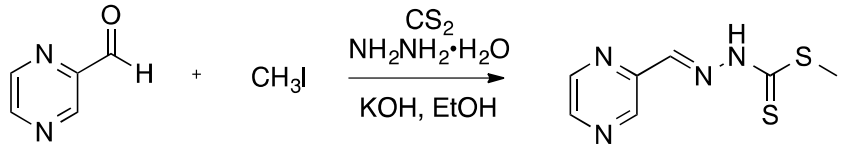

S10 **S7** **20**

Following Procedure A, pyrazine-2-carbaldehyde (0.20 g, 1.85 mmol) was converted to compound **16** (0.28 g, 1.31 mmol, 71%), a yellow solid (mp 174-176 °C decomp); t_R-HPLC: 17.0 min (95%); ^{1}H NMR (400 MHz, DMSO-d6) δ 9.10 (s, 1H), 8.53 – 8.48 (m, 2H), 8.21 (s, 1H), 2.51 (s, 3H); ^{13}C NMR (100 MHz, DMSO-d6) δ 200.06, 148.00, 145.16, 144.72, 143.95, 142.04, 16.97; FTIR υ_{max} 3112, 3058, 2994, 2918, 2794, 1602, 1547, 1507, 1461, 1405, 1347, 1296, 1275, 1180, 1168, 1149, 1112, 1065, 1045, 1011, 953, 907, 873, 834, 769, 745, 730, 700, 629, 604 cm^{-1}; ESI-MS (m/z) calcd for $C_7H_9N_4S_2$ $[M+H]^+$ 213.0269, found: 213.0267.

8.6. Methyl (*E*)-2-(thiazol-4-ylmethylene)hydrazine-1-carbodithioate (21

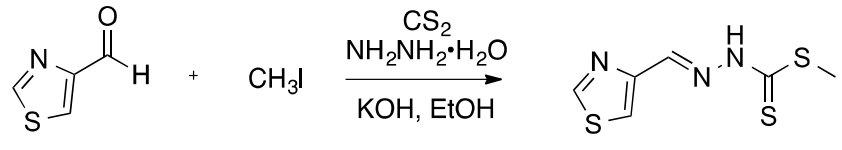

S11 **S7** **21**

Following Procedure A, thiazole-4-carbaldehyde (.15 g, 1.32 mmol) was converted to compound **21** (0.21 g, 0.98 mmol, 74%), a yellow solid (mp 173-175 °C decomp); t_R-HPLC: 17.1 min (97%); ^{1}H NMR (400 MHz, DMSO-d6) δ 9.20 (d, 1.90 Hz, 1H), 8.39 (s, 1H), 8.20 (d, 1.90 Hz, 1H), 2.52 (s, 3H); ^{13}C NMR (100 MHz, DMSO-d6) δ 198.54, 155.63, 150.55, 140.98, 121.58, 16.85; FTIR υ_{max} 3114, 3094, 3068, 2950, 2910, 2833, 1599, 1532, 1506, 1419, 1406, 1323, 1291, 1245, 1209, 1150, 1099, 1086, 1034, 969, 939, 880, 866, 835, 811, 758, 743, 678, 635, 604 cm^{-1}; ESI-MS (m/z) calcd for $C_6H_8N_3S_3$ $[M+H]^+$ 217.9880, found: 217.9878.

8.7. Methyl (*E*)-2-((1*H*-pyrazol-3-yl)methylene)hydrazine-1-carbodithioate (22)

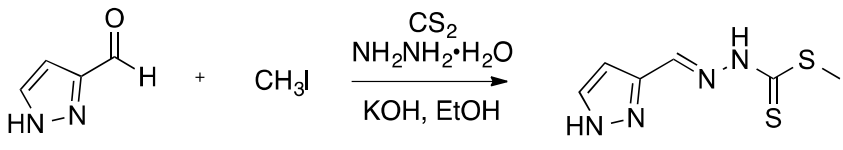

S12 **S7** **22**

Following Procedure A, 1*H*-pyrazole-3-carbaldehyde (0.20 g, 2.08 mmol) was converted to compound **22** (0.28 g, 1.41 mmol, 68%), a yellow solid (mp 173-175 °C decomp); t_R-HPLC:

16.1 min (93%); ^{1}H NMR (400 MHz, DMSO-d6) δ 8.29 (s, 1H), 7.83 (s, 1H), 6.60 (s, 1H), 2.51 (s, 3H); ^{13}C NMR (100 MHz, DMSO-d6) δ 197.77, 146.75, 141.93, 130.36, 102.36, 16.77; FTIR υ_{max} 3133, 3117, 3041, 2958, 2901, 1608, 1495, 1433, 1419, 1352, 1282, 1253, 1213, 1105, 1082, 1061, 1034, 994, 970, 900, 834, 824, 786, 769, 700, 644, 615, 553 cm^{-1}; ESI-MS (m/z) calcd for $C_6H_9N_4S_2$ $[M+H]^+$ 201.0269, found: 201.0270.

8.8. Methyl (*E*)-2-((4-chloro-1-methyl-1*H*-pyrazol-3-yl)methylene)hydrazine-1-carbodithioate (23)

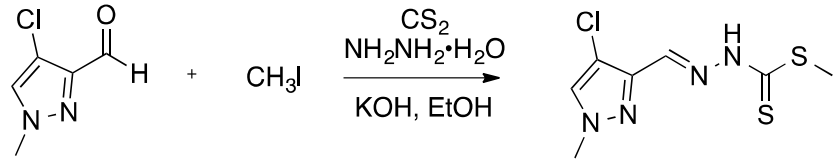

S13 **S7** **23**

Following Procedure A, 4-chloro-1-methyl-1*H*-pyrazole-3-carbaldehyde (0.16 g, 1.11 mmol) was converted to compound **23** (0.19 g, 0.07 mmol, 68%), a yellow solid (mp 177-179 °C); t_R-HPLC: 16.9 min (99%); ^{1}H NMR (500 MHz, DMSO-d6) δ 8.21 (s, 1H), 8.05 (s, 1H), 3.85 (s, 3H), 2.49 (s, 3H); ^{13}C NMR (125 MHz, DMSO-d6) δ 198.68, 141.17, 139.00, 131.50, 107.79, 39.72, 16.87; FTIR υ_{max} 3121, 3017, 2961, 2916, 2839, 1610, 1521, 1514, 1466, 1425, 1333, 1303, 1289, 1168, 1113, 1094, 1037, 1013, 962, 927, 828, 798, 734, 649, 622 cm^{-1}; ESI-MS (m/z) calcd for $C_7H_{10}N_4S_2Cl$ $[M+H]^+$ 249.0035, found: 249.0034.

8.9. Methyl (*E*)-2-((6-methylpyridin-2-yl)methylene)hydrazine-1-carbodithioate (24)

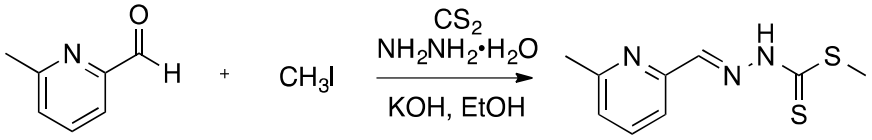

S14 **S7** **24**

Following Procedure A, 6-methylpicolinaldehyde (0.30 g, 2.48 mmol) was converted to compound **24** (0.42 g, 1.88 mmol, 76%), a yellow solid (mp 174-176 °C decomp); t_R-HPLC: 17.3 min (92%); ^{1}H NMR (500 MHz, DMSO-d6) δ 8.20 (s, 1H), 7.78 – 7.70 (m, 2H), 7.29 (d, *J* = 7.2 Hz, 1H), 2.52 (s, 3H), 2.48 (s, 3H); ^{13}C NMR (125 MHz, DMSO-d6) δ 199.21, 158.25, 151.72, 146.70, 137.21, 124.27, 117.11, 23.81, 16.82; FTIR υ_{max} 3085, 2997, 2917, 2775, 1584, 1527, 1455, 1293, 1266, 1248, 1159, 1107, 1093, 1058, 991, 963, 950, 920, 905, 797, 788, 736, 730, 664, 607 cm^{-1}; ESI-MS (m/z) calcd for $C_9H_{12}N_3S_2$ $[M+H]^+$ 226.0473, found: 226.0475.

8.10. Methyl (*E*)-2-((3-methylpyridin-2-yl)methylene)hydrazine-1-carbodithioate (25)

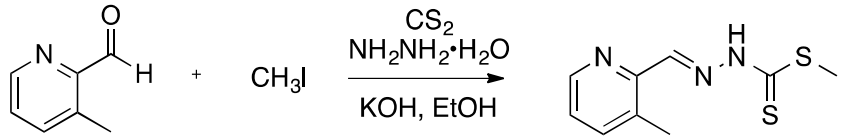

S15 **S7** **25**

Following Procedure A, 3-methylpicolinaldehyde (0.25 g, 2.06 mmol) was converted to compound **25** (0.31 g, 1.40 mmol, 68%), a yellow solid (mp 174-176 °C decomp); t_R-HPLC: 17.3 min (96%); ^{1}H NMR (500 MHz, DMSO-d6) δ 8.49 (d, *J* = 4.8Hz, 1H), 8.42 (s, 1H), 7.71 (d, *J* = 7.5 Hz, 1H), 7.32 (dd, *J* = 4.8, 7.5 Hz, 1H), 2.58 (s, 3H), 2.52 (s, 3H); ^{13}C NMR (125 MHz, DMSO-d6) δ 199.21, 149.51, 149.05, 147.14, 139.49, 133.56, 123.82, 21.00, 16.93; FTIR υ_{max} 3401, 3088, 2914, 2793, 1566, 1524, 1450, 1416, 1400, 1309, 1286, 1271, 1216, 1189, 1132, 1101, 1060, 1043, 1001, 959, 938, 899, 824, 794, 771, 754, 725, 665, 610, 578 cm^{-1}; ESI-MS (m/z) calcd for $C_9H_{12}N_3S_2$ $[M+H]^+$ 226.0473, found: 226.0475.

8.11. Methyl (*E*)-2-((5-bromopyridin-2-yl)methylene)hydrazine-1-carbodithioate (26)

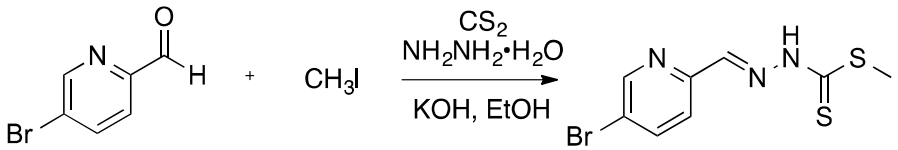

S16 **S7** **26**

Following Procedure A, 5-bromopicolinaldehyde (0.15 g, 0.81 mmol) was converted to compound **26** (0.17 g, 0.58 mmol, 72%), a yellow solid (mp 177-179 °C decomp); t_R-HPLC: 17.4 min (99%); ^{1}H NMR (500 MHz, DMSO-d6) δ 8.15 (s, 1H), 7.90 (d, *J* = 7.4 Hz, 1H), 7.83 (t, *J* = 7.4 Hz, 1H), 7.70 (d, *J* = 7.4 Hz, 1H), 2.53 (s, 3H); ^{13}C NMR (125 MHz, DMSO-d6) δ 199.75, 153.57, 144.42, 141.22, 140.30, 129.02, 119.39, 16.87; FTIR υ_{max} 3121, 3073, 2983, 2936, 2916, 2842, 1572, 1550, 1519, 1428, 1411, 1334, 1311, 1294, 1255, 1159, 1122, 1106, 1053, 990, 983, 961, 952, 930, 890, 791, 724, 714, 649, 605 cm^{-1}; ESI-MS (m/z) calcd for $C_8H_9N_3S_2Br$ $[M+H]^+$ 289.9421, found: 289.9414.

8.12. Methyl (*E*)-2-((6-bromopyridin-2-yl)methylene)hydrazine-1-carbodithioate (27)

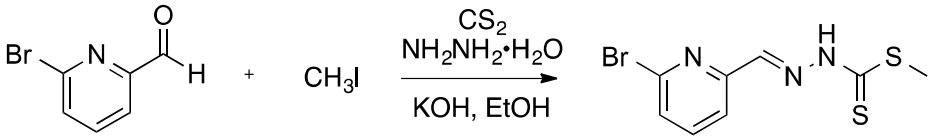

S17 **S7** **27**

Following Procedure A, 6-bromopicolinaldehyde (0.15 g, 0.81 mmol) was converted to compound **27** (0.16 g, 0.56 mmol, 70%), a yellow solid (mp 177-179 °C decomp); t_R-HPLC: 17.4 min (98%); ^{1}H NMR (500 MHz, DMSO-d6) δ 8.76 (d, *J* = 2.2 Hz, 1H), 8.23 (s, 1H), 8.15 (dd, *J* = 2.2, 8.5 Hz, 1H), 7.85 (d, *J* = 8.5 Hz, 1H), 2.54 (s, 3H); ^{13}C NMR (125 MHz, DMSO-d6) δ 199.54, 151.14, 150.57, 145.20, 139.77, 121.49, 109.11, 16.85; FTIR υ_{max} 3121, 2989, 2959, 2910, 2846, 1565, 1519, 1461, 1307, 1281, 1257, 1215, 1123, 1107, 1089, 1051, 1006, 970, 961, 933, 872, 829, 735, 707, 650, 637, 609 cm^{-1}; ESI-MS (m/z) calcd for $C_8H_9N_3S_2Br$ $[M+H]^+$ 289.9421, found: 289.9417.

8.13. Methyl (*E*)-2-((3-fluoropyridin-2-yl)methylene)hydrazine-1-carbodithioate (28)

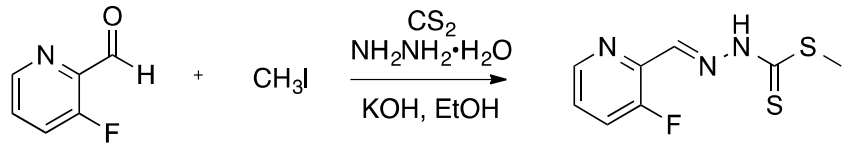

S18 **S7** **28**

Following Procedure A, 3-fluoropicolinaldehyde (0.10 g, 0.80 mmol) was converted to compound **28** (0.11 g, 0.49 mmol, 62%), a yellow solid (mp 176-178 °C decomp); t_R-HPLC: 17.2 min (98%); ^{1}H NMR (500 MHz, DMSO-d6) δ 8.55 – 8.46 (m, 1H), 8.41 – 8.34 (m, 1H), 7.86 – 7.75 (m, 1H), 7.58 – 7.48 (m, 1H), 2.49 (s, 3H); ^{13}C NMR (125 MHz, DMSO-d6) δ 199.95, 157.99 (d, ^1J = 262 Hz), 146.09, 142.50, 139.81, 126.42, 124.81 (d, ^2J = 21 Hz), 16.91; FTIR υ_{max} 3127, 3054, 3028, 2991, 2955, 2921, 2854, 1593, 1558, 1523, 1463, 1449, 1416, 1324, 1288, 1271, 1239, 1165, 1119, 1101, 1068, 1047, 956, 930, 892, 873, 811, 801, 771, 732, 709, 662, 625, 593, 585 cm^{-1}; ESI-MS (m/z) calcd for $C_8H_9N_3S_2F$ $[M+H]^+$ 230.0222, found: 230.0220.

8.14. Methyl (*E*)-2-((1*H*-indol-3-yl)methylene)hydrazine-1-carbodithioate (29)

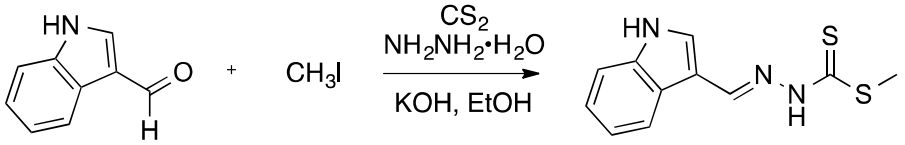

S19 **S7** **29**

Following Procedure A, 1*H*-indole-3-carbaldehyde (0.10 g, 0.69 mmol) was converted to compound **29** (0.11 g, 0.45 mmol, 65%), a yellow solid (mp 178-180 °C decomp); t_R-HPLC: 16.7 min (96%); ^{1}H NMR (400 MHz, DMSO-d6) δ 8.45 (s, 1H), 8.29 (d, *J* = 7.2 Hz, 1H), 7.94 (d, *J* = 2.8 Hz, 1H), 7.46 (d, *J* = 7.4 Hz, 1H), 7.26 – 7.16 (m, 2H), 2.56 (s, 3H); ^{13}C NMR (100 MHz, DMSO-d6) δ 195.02, 143.73, 137.16, 132.67, 124.01, 123.00, 121.94, 121.08, 112.08, 111.01, 16.74; FTIR υ_{max} 3376, 3125, 3105, 3061, 2969, 2930, 2885, 1601, 1575, 1532, 1447, 1431, 1307, 1288, 1245, 1136, 1100, 1080, 1031, 1017, 1000, 996, 969, 943, 831, 803, 746, 637, 611 cm^{-1}; ESI-MS (m/z) calcd for $C_{11}H_{12}N_3S_2$ $[M+H]^+$ 250.0473, found: 250.0477.

8.15. Methyl (*E*)-2-((1-methyl-1*H*-indol-2-yl)methylene)hydrazine-1-carbodithioate (30)

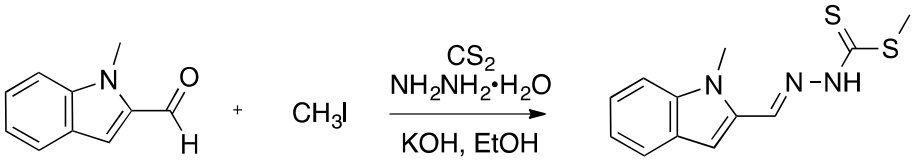

S20 **S7** **30**

Following Procedure A, 1-methyl-1*H*-indole-2-carbaldehyde (0.10 g, 0.63 mmol) was converted to compound **30** (0.10 g, 0.38 mmol, 61%), a yellow solid (mp 178-180 °C decomp); t_R-HPLC: 17.1 min (94%); ^{1}H NMR (400 MHz, DMSO-d6) δ 8.36 (s, 1H), 7.61 (d, *J* = 7.9 Hz, 1H), 7.54 (d, *J* = 8.4 Hz, 1H), 7.32 – 7.26 (m, 1H), 7.12 – 7.07 (m, 1H), 7.00 (s, 1H), 4.07 (s, 3H), 2.55 (s, 3H); ^{13}C NMR (100 MHz, DMSO-d6) δ 197.36, 139.91, 139.68, 132.34, 126.76, 124.19, 121.30, 120.15, 110.27, 110.21, 32.21, 16.84; FTIR υ_{max} 3139, 3041, 2969, 2910, 1594, 1521, 1465, 1402, 1361, 1304, 1188, 1147, 1125, 1091, 1040, 962, 933, 913, 870, 813, 749, 740, 648, 625, 596 cm^{-1}; ESI-MS (m/z) calcd for $C_{12}H_{14}N_3S_2$ $[M+H]^+$ 264.0629, found: 264.0631.

8.16. 2-Oxo-2-(phenylamino)ethyl (*E*)-2-(pyridin-2-ylmethylene)hydrazine-1-carbodithioate (31)

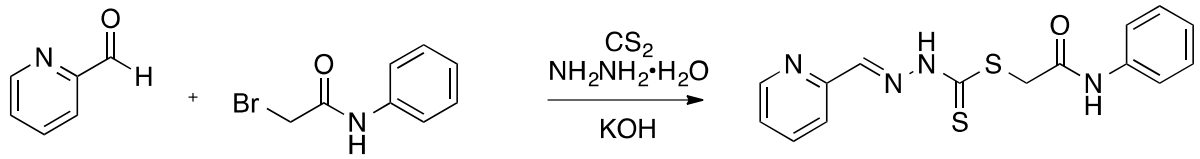

S6 **S21** **31**

Following the sequence of Procedure B, C and D, picolinaldehyde (0.40 g, 3.73 mmol) was converted to compound **31** (0.84 g, 2.54 mmol, 68%), a yellow solid (mp 178-180 °C decomp); t_R-HPLC: 19.9 min (99%); ^{1}H NMR (500 MHz, DMSO-d6) δ 10.30 (s, 1H), 8.66 – 8.62 (m, 1H), 8.29 (s, 1H), 7.99 – 7.95 (m, 1H), 7.94 – 7.88 (m, 1H), 7.59 (d, *J* = 7.8 Hz, 2H), 7.49 – 7.45 (m, 1H), 7.34 – 7.28 (m, 2H), 7.05 (t, *J* = 7.4 Hz, 1H), 4.22 (s, 2H); ^{13}C NMR (100 MHz, DMSO-d6) δ 197.41, 165.55, 152.22, 149.87, 146.81, 139.02, 137.13, 128.78, 125.05, 123.36, 120.18, 119.07, 38.83; FTIR υ_{max} 3244, 3121, 3095, 3055, 3011, 2927, 2836, 1662, 1602, 1526, 1457, 1439, 1369, 1318, 1286, 1251, 1150, 1112, 1046, 999, 966, 933, 877, 779, 752, 680, 633, 603, 554 cm^{-1}; ESI-MS (m/z) calcd for $C_{15}H_{15}N_4OS_2$ $[M+H]^+$ 331.0687, found: 331.0682.

8.17. 2-Oxo-2-(*p*-tolylamino)ethyl (*E*)-2-(pyridin-2-ylmethylene)hydrazine-1-carbodithioate (32)

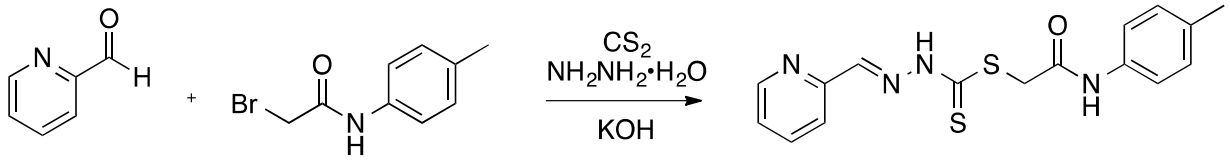

S6 **S22** **32**

Following the sequence of Procedure B, C and D, picolinaldehyde (0.40 g, 3.73 mmol) was converted to compound **32** (0.86 g, 2.50 mmol, 67%), a yellow solid (mp 178-180 °C decomp); t_R-HPLC: 20.0 min (96%); ^{1}H NMR (400 MHz, DMSO-d6) δ 10.22 (s, 1H), 8.66 – 8.62 (m, 1H), 8.29 (s, 1H), 7.99-7.95 (m, 1H), 7.94 – 7.88 (m, 1H), 7.47 (d, *J* = 8.5 Hz, 2H), 7.11 (d, *J* = 8.5 Hz, 2H), 4.19 (s, 2H), 2.25 (s, 3H); ^{13}C NMR (100 MHz, DMSO-d6) δ 197.43, 165.28, 152.22, 149.87, 146.80, 137.13, 136.52, 132.28, 129.14, 125.05, 120.18, 119.09, 38.88, 20.45; FTIR υ_{max} 3246, 3185, 3114, 3033, 2916, 1655, 1596, 1526, 1468, 1369, 1318, 1285, 1251, 1162, 1113,

1048, 999, 932, 877, 815, 796, 680, 634, 601, 576 cm^{-1}; ESI-MS (m/z) calcd for $C_{16}H_{16}N_4ONaS_2$ $[M+Na]^+$ 367.0663, found: 367.0654.

8.18. 2-((4-(*tert*-Butyl)phenyl)amino)-2-oxoethyl (*E*)-2-(pyridin-2-ylmethylene)hydrazine-1-carbodithioate (33)

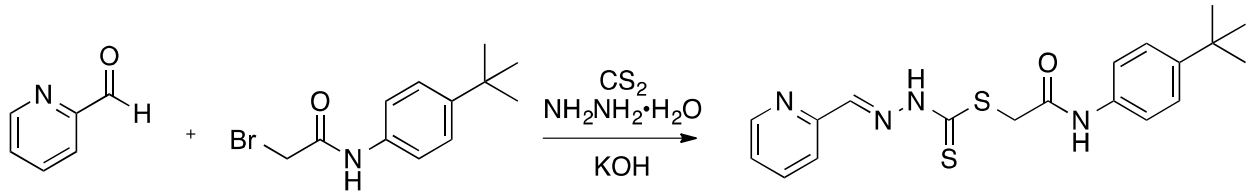

S6 **S23** **33**

Following the sequence of Procedure B, C and D, picolinaldehyde (0.40 g, 3.73 mmol) was converted to compound **33** (0.94 g, 2.42 mmol, 65%), a yellow solid (mp 178-180 °C decomp); t_R-HPLC: 20.2 min (97%); ^{1}H NMR (500 MHz, DMSO-d6) δ 10.23 (s, 1H), 8.66-8.62 (m, 1H), 8.29 (s, 1H), 7.98 – 7.89 (m, 2H), 7.52 – 7.45 (m, 3H), 7.32 (d, *J* = 8.7 Hz, 2H), 4.19 (s, 2H), 1.25 (s, 9H); ^{13}C NMR (125 MHz, DMSO-d6) δ 197.47, 165.35, 152.24, 149.89, 146.80, 145.74, 137.15, 136.45, 125.39, 125.07, 120.20, 118.92, 38.79, 34.04, 31.21; FTIR υ_{max} 3261, 3114, 2960, 2864, 1662, 1601, 1558, 1538, 1489, 1394, 1318, 1283, 1261, 1193, 1110, 1047, 1000, 967, 927, 876, 828, 773, 740, 680, 659, 633, 598 cm^{-1}; ESI-MS (m/z) calcd for $C_{19}H_{23}N_4OS_2$ $[M+H]^+$ 387.1313, found: 387.1313.

8.19. 2-((4-Methoxyphenyl)amino)-2-oxoethyl (*E*)-2-(pyridin-2-ylmethylene)hydrazine-1-carbodithioate (34)

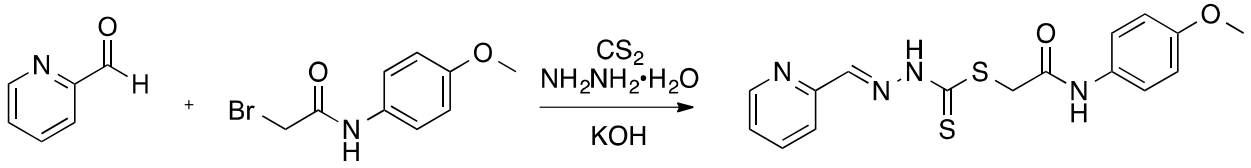

S6 **S24** **34**

Following the sequence of Procedure B, C and D, picolinaldehyde (0.15 g, 1.40 mmol) was converted to compound **34** (0.35 g, 0.97 mmol, 69%), a yellow solid (mp 177-179 °C decomp); t_R-HPLC: 19.8 min (97%); ^{1}H NMR (400 MHz, DMSO-d6) δ 10.37 (s, 1H), 8.66-8.62 (m, 1H), 8.28 (s, 1H), 7.99-7.86 (m, 2H), 7.65 – 7.55 (m, 2H), 7.50 – 7.43 (m, 1H), 7.20-7.10 (m, 2H), 4.20 (s, 2H), 3.33 (s, 3H); ^{13}C NMR (100 MHz, DMSO-d6) δ 197.42, 165.03, 155.29, 152.24, 149.88, 146.79, 137.17, 132.17, 125.05, 120.64, 120.19, 113.89, 55.16, 38.76; FTIR υ_{max} 3420,

3256, 3095, 3003, 2951, 2833, 1661, 1532, 1510, 1464, 1434, 1359, 1143, 1109, 1085, 1043, 1086, 1043, 1025, 998, 970, 970, 872, 829, 776, 678, 632, 600 cm^{-1}; ESI-MS (m/z) calcd for $C_{16}H_{16}N_4O_2NaS_2$ $[M+Na]^+$ 383.0612, found: 383.0606.

8.20. 2-((4-Fluorophenyl)amino)-2-oxoethyl (*E*)-2-(pyridin-2-ylmethylene)hydrazine-1-carbodithioate (35)

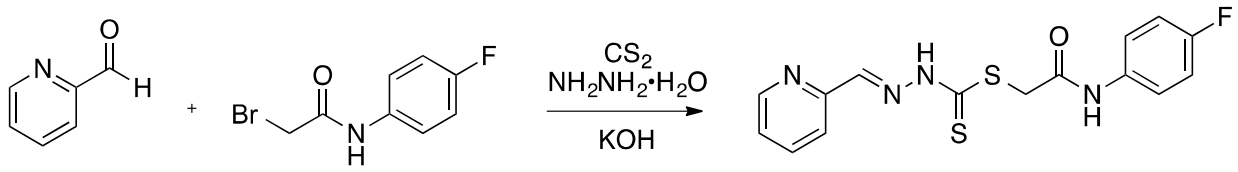

S6 **S25** **35**

Following the sequence of Procedure B, C and D, picolinaldehyde (0.15 g, 1.40 mmol) was converted to compound **35** (0.29 g, 0.84 mmol, 60%), a yellow solid (mp 178-180 °C decomp); t_R-HPLC: 19.8 min (98%); ^{1}H NMR (500 MHz, DMSO-d6) δ 10.36 (s, 1H), 8.64 (d, *J* = 4.4 Hz, 1H), 8.29 (s, 1H), 7.98 – 7.88 (m, 2H), 7.61 (dd, *J* = 8.7, 5.0 Hz, 2H), 7.49 – 7.44 (m, 1H), 7.15 (t, *J* = 8.8 Hz, 2H), 4.21 (s, 2H); ^{13}C NMR (125 MHz, DMSO-d6) δ 197.35, 165.52, 158.03 (d, ^1J = 239 Hz), 152.21, 149.86, 146.83, 137.10, 135.39, 125.03, 120.85 (d, ^3J = 7.7 Hz), 120.18, 115.34 (d, ^2J = 22 Hz), 38.69; FTIR υ_{max} 3243, 2918, 2849, 1654, 1584, 1526, 1505, 1468, 1374, 1316, 1284, 1265, 1209, 1164, 1151, 1115, 1048, 999, 972, 933, 887, 833, 804, 781, 681, 634, 602 cm^{-1}; ESI-MS (m/z) calcd for $C_{15}H_{14}FN_4OS_2$ $[M+H]^+$ 349.0593, found: 349.0590.

8.21. 2-((3-bromophenyl)amino)-2-oxoethyl (*E*)-2-(pyridin-2-ylmethylene)hydrazine-1-carbodithioate (36)

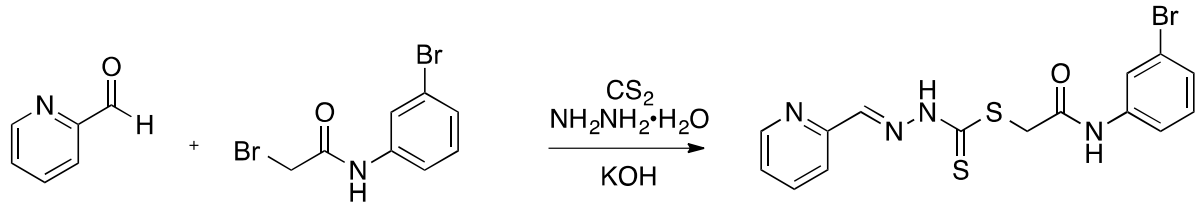

S6 **S26** **36**

Following the sequence of Procedure B, C and D, picolinaldehyde (0.15 g, 1.40 mmol) was converted to compound **36** (0.36 g, 0.88 mmol, 63%), a yellow solid (mp 178-180 °C decomp); t_R-HPLC: 20.0 min (99%); ^{1}H NMR (500 MHz, DMSO-d6) δ 10.49 (s, 1H), 8.64 (d, *J* = 4.6 Hz, 1H), 8.29 (s, 1H), 7.98 – 7.88 (m, 3H), 7.52 – 7.44 (m, 2H), 7.30 – 7.22 (m, 2H), 4.23 (s, 2H); ^{13}C NMR (125 MHz, DMSO-d6) 197.32, 166.05, 152.20, 149.86, 146.87, 140.56, 137.10,

130.80, 125.98, 121.59, 121.43, 120.19, 117.86, 38.70; FTIR υ_{max} 3274, 3097, 1663, 1593, 1523, 1466, 1436, 1422, 1367, 1318, 1285, 1262, 1247, 1199, 1163, 1146, 1109, 1085, 1067, 1044, 999, 969, 930, 911, 893, 879, 866, 776, 741, 679, 666, 632, 603, 580 cm^{-1}; ESI-MS (m/z) calcd for $C_{15}H_{14}BrN_4OS_2$ $[M+H]^+$ 408.9792, found: 408.9792.

8.22. 2-Oxo-2-(*p*-tolylamino)ethyl (*E*)-2-((6-methylpyridin-2-yl)methylene)hydrazine-1-carbodithioate (37)

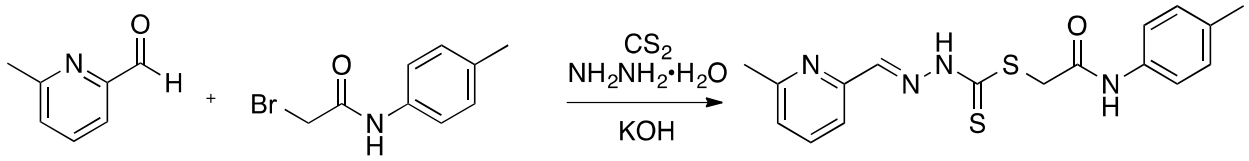

S14 **S22** **37**

Following the sequence of Procedure B, C and D, 6-methylpicolinaldehyde (0.15 g, 1.24 mmol) was converted to compound **37** (0.31 g, 0.87 mmol, 70%), a yellow solid (mp 178-180 °C decomp); t_R-HPLC: 20.1 min (94%); ^{1}H NMR (500 MHz, $CDCl_3$) δ 8.74 (s, 3H), 7.77 (t, *J* = 7.7 Hz, 1H), 7.37 (d, *J* = 8.2 Hz, 2H), 7.32 – 7.24 (m, 3H), 7.07 (d, *J* = 8.2 Hz, 2H), 4.20 (s, 2H), 2.68 (s, 3H), 2.27 (s, 3H); ^{13}C NMR (125 MHz, $CDCl_3$) δ 199.65, 167.02, 158.41, 150.93, 138.37, 137.24, 135.57, 134.06, 129.57, 125.05, 123.83, 120.20, 37.79, 24.57, 21.08; FTIR υ_{max} 3268, 2916, 1649, 1598, 1584, 1542, 1511, 1475, 1457, 1407, 1358, 1323, 1280, 1238, 1200, 1178, 1156, 1109, 1037, 999, 984, 970, 945, 927, 917, 866, 809, 787, 710, 683, 662, 621, 585 cm^{-1}; ESI-MS (m/z) calcd for $C_{17}H_{19}N_4OS_2$ $[M+H]^+$ 359.1000, found: 359.1002.

8.23. 2-((4-(*tert*-Butyl)phenyl)amino)-2-oxoethyl (*E*)-2-((6-methylpyridin-2-yl)methylene)hydrazine-1-carbodithioate (38)

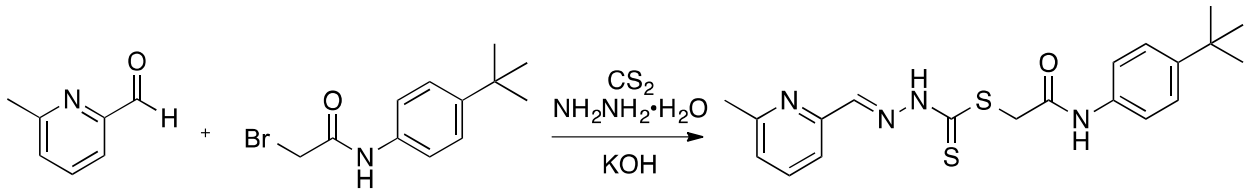

S14 **S23** **38**

Following the sequence of Procedure B, C and D, 6-methylpicolinaldehyde (0.15 g, 1.24 mmol) was converted to compound **38** (0.34 g, 0.85 mmol, 69%), a yellow solid (mp 178-180 °C decomp); t_R-HPLC: 20.4 min (99%); ^{1}H NMR (500 MHz, $CDCl_3$) δ 8.76 (s, 1H), 7.76 (t, *J* = 7.8 Hz, 1H), 7.41 (d, *J* = 8.5 Hz, 2H), 7.31 – 7.27 (m, 4H), 7.27-7.24 (m, 1H), 4.20 (s, 2H), 2.67 (s, 3H), 1.26 (s, 9H); ^{13}C NMR (125 MHz, $CDCl_3$) δ 199.59, 167.07, 158.38, 150.91, 147.43,

138.36, 137.22, 135.46, 125.89, 125.03, 123.82, 119.96, 37.77, 34.54, 31.54, 24.55; FTIR υ_{max} 3282, 3114, 2960, 2903, 2865, 1661, 1599, 1518, 1476, 1407, 1362, 1319, 1304, 1269, 1249, 1159, 1104, 1047, 994, 909, 834, 786, 733, 709, 667 cm^{-1}; ESI-MS (m/z) calcd for $C_{20}H_{25}N_4OS_2$ $[M+H]^+$ 401.1470, found: 401.1469.

8.24. 2-((4-Methoxyphenyl)amino)-2-oxoethyl (*E*)-2-((6-methylpyridin-2-yl)methylene)hydrazine-1-carbodithioate (39)

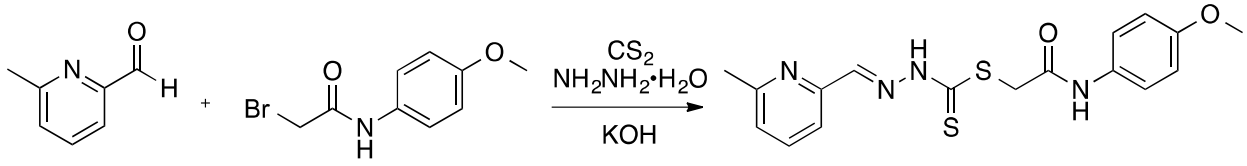

S14 **S24** **39**

Following the sequence of Procedure B, C and D, 6-methylpicolinaldehyde (0.15 g, 1.24 mmol) was converted to compound **39** (0.31 g, 0.84 mmol, 68%), a yellow solid (mp 178-180 °C decomp); t_R-HPLC: 19.9 min (99%); ^{1}H NMR (500 MHz, DMSO-d6) δ 10.14 (s, 1H), 8.22 (s, 1H), 7.80 – 7.74 (m, 2H), 7.48 (d, *J* = 9.0 Hz, 2H), 7.34 – 7.27 (m, 1H), 6.87 (d, *J* = 9.0 Hz, 2H), 4.16 (s, 2H), 3.70 (s, 3H), 2.49 (s, 3H); ^{13}C NMR (125 MHz, DMSO-d6) δ 197.27, 165.00, 158.30, 155.27, 151.59, 147.02, 137.27, 132.14, 124.39, 120.62, 117.27, 113.86, 55.14, 38.71, 23.81; FTIR υ_{max} 3260, 3063, 2953, 2834, 1669, 1510, 1455, 1410, 1290, 1268, 1244, 1168, 1159, 1106, 1060, 1026, 992, 968, 924, 825, 734, 786, 709, 665, 610 cm^{-1}; ESI-MS (m/z) calcd for $C_{17}H_{19}N_4O_2S_2$ $[M+H]^+$ 375.0949, found: 375.0949.

8.25. 2-Oxo-2-(*p*-tolylamino)ethyl (*E*)-2-((3-methylpyridin-2-yl)methylene)hydrazine-1-carbodithioate (40)

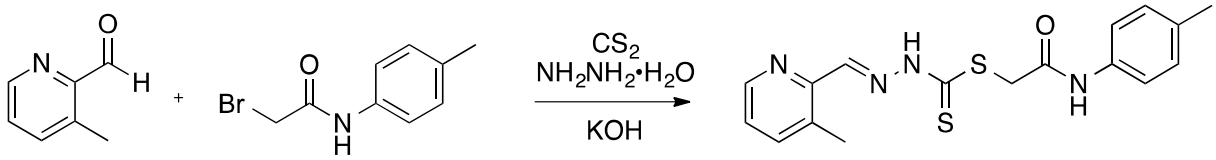

S15 **S22** **40**

Following the sequence of Procedure B, C and D, 3-methylpicolinaldehyde (0.12 g, 0.99 mmol) was converted to compound **40** (0.22 g, 0.61 mmol, 62%), a yellow solid (mp 178-180 °C decomp); t_R-HPLC: 20.1 min (99%); ^{1}H NMR (500 MHz, DMSO-d6) δ 10.19 (s, 1H), 8.52 (d, *J* = 4.5 Hz, 1H), 8.46 (s, 1H), 7.75 (d, *J* = 7.4 Hz, 1H), 7.47 (d, *J* = 7.8 Hz, 2H), 7.36 (dd, *J* = 4.5, 7.4 Hz, 1H), 7.11 (d, *J* = 7.8 Hz, 2H), 4.20 (s, 2H), 2.63 (s, 3H), 2.25 (s, 3H); ^{13}C NMR (125

MHz, DMSO-d6) δ 197.33, 165.33, 149.42, 149.39, 147.20, 139.53, 136.53, 133.69, 132.23, 129.10, 123.94, 119.07, 38.80, 20.98, 20.42; FTIR υ_{max} 3273, 3115, 2917, 1661, 1597, 1514, 1447, 1405, 1372, 1354, 1313, 1275, 1247, 1213, 1192, 1162, 1124, 1105, 1061, 1040, 1000, 963, 902, 885, 812, 754, 688, 667, 615, 579 cm^{-1}; ESI-MS (m/z) calcd for $C_{17}H_{19}N_4OS_2$ $[M+H]^+$ 359.1000, found: 359.1003.

8.26. 2-Oxo-2-(*p*-tolylamino)ethyl (*E*)-2-((3-fluoropyridin-2-yl)methylene)hydrazine-1-carbodithioate (41)

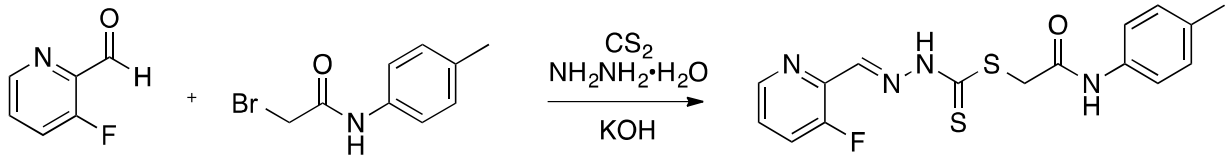

S18 **S22** **41**

Following the sequence of Procedure B, C and D, 3-fluoropicolinaldehyde (0.15 g, 1.20 mmol) was converted to compound **41** (0.27 g, 0.74 mmol, 62%), a yellow solid (mp 178-180 °C decomp); t_R-HPLC: 19.8 min (97%); ^{1}H NMR (500 MHz, DMSO-d6) δ 10.19 (s, 1H), 8.54 (d, *J* = 4.3 Hz, 1H), 8.41 (s, 1H), 7.88 – 7.81 (m, 1H), 7.60-7.54 (m, 1H), 7.47 (d, *J* = 8.2 Hz, 2H), 7.11 (d, *J* = 8.2 Hz, 2H), 4.18 (s, 2H), 2.25 (s, 3H); ^{13}C NMR (125 MHz, DMSO-d6) δ 198.44, 165.59, 158.52 (d, ^1J = 265 Hz), 146.61, 143.22, 140.13 (d, ^2J = 8.1 Hz), 136.96, 132.70, 129.57, 126.98, 125.31 (d, ^2J = 18.4 Hz), 119.55, 39.31, 20.88; ; FTIR υ_{max} 3267, 3088, 2918, 2832, 1651, 1597, 1520, 1448, 1403, 1304, 1291, 1266, 1227, 1186, 1117, 1092, 963, 933, 924, 907, 886, 858, 810, 787, 746, 706, 691, 656, 617, 573 cm^{-1}; ESI-MS (m/z) calcd for $C_{16}H_{15}FN_4ONaS_2$ $[M+Na]^+$ 385.0569, found: 385.0562.

8.27. 2-((4-(*tert*-Butyl)phenyl)amino)-2-oxoethyl (*E*)-2-((3-fluoropyridin-2-yl)methylene)hydrazine-1-carbodithioate (42)

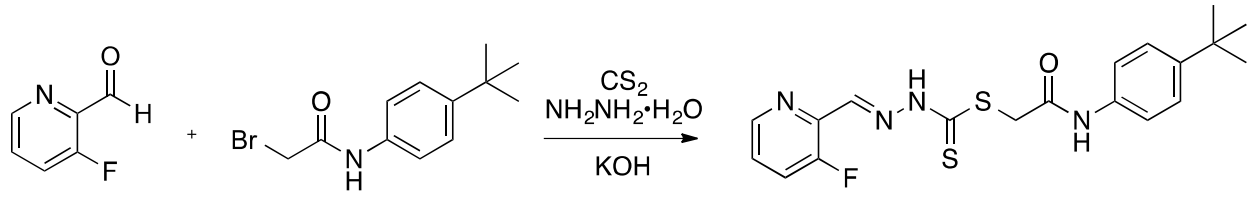

S18 **S23** **42**

Following the sequence of Procedure B, C and D, 3-fluoropicolinaldehyde (0.15 g, 1.20 mmol) was converted to compound **42** (0.29 g, 0.72 mmol, 60%), a yellow solid (mp 178-180 °C decomp); t_R-HPLC: 20.0 min (99%); ^{1}H NMR (500 MHz, DMSO-d6) δ 10.21 (s, 1H), 8.56-8.51

(m, 1H), 8.41 (s, 1H), 7.88-7.80(m, 1H), 7.60 –7.54 (m, 1H), 7.53-7.46 (m, 2H), 7.35-7.28 (m, 2H), 4.18 (s, 2H), 1.26 (s, 9H); ^{13}C NMR (125 MHz, DMSO-d6) δ 198.04, 165.32, 158.07 (D, ^{1}J = 266 Hz), 146.15, 145.66, 142.78, 139.67 (d, ^{2}J = 7.7 Hz), 136.43, 126.56, 125.34, 124.86 (d, ^{2}J = 18 Hz), 118.88, 38.82, 33.99, 31.17; FTIR υ_{max} 3279, 3063, 2957, 2865, 1662, 1599, 1529, 1464, 1408, 1359, 1319, 1285, 1250 1192, 1115, 1039, 958, 873, 828, 801, 712, 663, 595 cm^{-1}; ESI-MS (m/z) calcd for $C_{19}H_{21}FN_4OS_2Na$ $[M+Na]^+$ 427.1039, found: 427.1027.

8.28. 2-((4-Methoxyphenyl)amino)-2-oxoethyl (*E*)-2-((3-fluoropyridin-2-yl)methylene)hydrazine-1-carbodithioate (43)

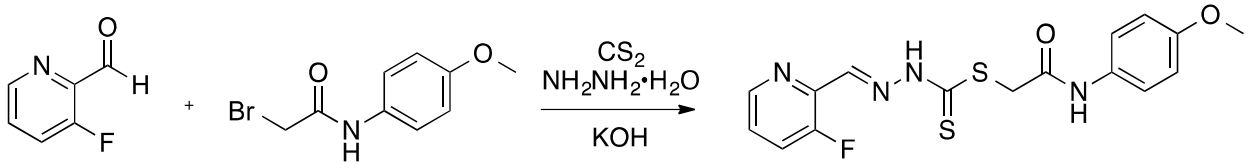

S18 **S24** **43**

Following the sequence of Procedure B, C and D, 3-fluoropicolinaldehyde (0.15 g, 1.20 mmol) was converted to compound **43** (0.29 g, 0.77 mmol, 64%), a yellow solid (mp 178-180 °C decomp); t_R-HPLC: 19.8 min (96%); ^{1}H NMR (400 MHz, DMSO-d6) δ 10.17 (s, 1H), 8.54 (d, *J* = 4.3 Hz, 1H), 8.41 (s, 1H), 7.88 – 7.80 (m, 1H), 7.60 – 7.54 (m, 1H), 7.50 (d, *J* = 9.0 Hz, 2H), 6.88 (d, *J* = 9.0 Hz, 2H), 4.17 (s, 2H), 3.71 (s, 3H); ^{13}C NMR (100 MHz, DMSO-d6) δ 198.06, 165.08, 158.11 (d, *J* = 265 Hz), 155.29, 146.20, 142.83, 189.69 (d, ^{2}J = 7.8 Hz), 132.20, 126.62, 124.90 (d, ^{2}J = 18 Hz), 120.66, 113.89, 55.17, 38.83; FTIR υ_{max} 3290, 3078, 2932, 2835, 1668, 1599, 1512, 1449, 1412, 1357, 1303, 1289, 1269, 1243, 1230, 1190, 1119, 1047, 1025, 964, 924, 907, 884, 825, 813, 801, 787, 746, 713, 699, 658, 620 cm^{-1}; ESI-MS (m/z) calcd for $C_{16}H_{16}FN_4O_2S_2$ $[M+H]^+$ 379.0698, found: 379.0696.

8.29. 2-Oxo-2-((4-(trifluoromethyl)phenyl)amino)ethyl (*E*)-2-((3-fluoropyridin-2-yl)methylene)hydrazine-1-carbodithioate (44)

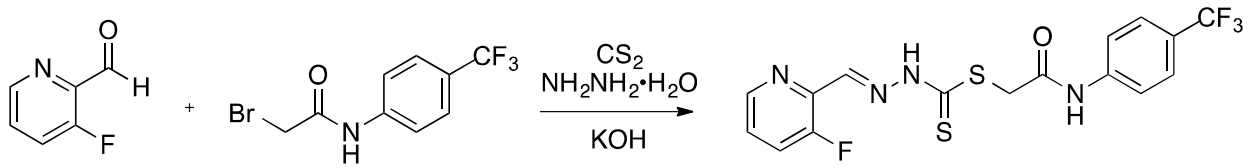

S18 **S27** **44**

Following the sequence of Procedure B, C and D, 3-fluoropicolinaldehyde (0.15 g, 1.20 mmol) was converted to compound **44** (0.28 g, 0.67 mmol, 56%), a yellow solid (mp 178-180 °C

decomp); t_R-HPLC: 19.5 min (93%); ^{1}H NMR (400 MHz, DMSO-d6) δ 10.68 (s, 1H), 8.56 – 8.52 (m, 1H), 8.42 (s, 1H), 7.89 – 7.82 (m, 1H), 7.81 (d, *J* = 8.7 Hz, 2H), 7.69 (d, *J* = 8.7 Hz, 2H), 4.24 (s, 2H); ^{13}C NMR (125 MHz, DMSO-d6) δ 197.89, 166.35, 158.09 (d, ^1J = 265 Hz), 146.13, 142.88, 142.55, 139.68, 139.61, 126.58, 126.10, 124.94, 124.79, 123.45, 123.27, 118.95, 38.79; FTIR υ_{max} 3251, 3120, 3052, 1684, 1609, 1545, 1520, 1447, 1412, 1322, 1252, 1167, 1070, 1047, 1023, 910, 843, 816, 712, 661, 630, 603 cm^{-1}; ESI-MS (m/z) calcd for $C_{16}H_{13}F_4N_4OS_2$ $[M+H]^+$ 417.0467, found: 417.0466.

8.30. 2-Oxo-2-(*p*-tolylamino)ethyl (*E*)-2-((6-bromopyridin-2-yl)methylene)hydrazine-1-carbodithioate (45)

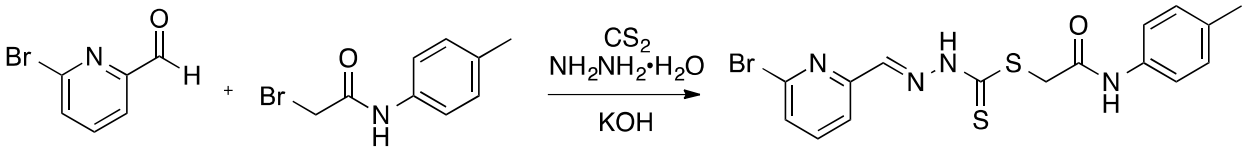

S17 **S22** **45**

Following the sequence of Procedure B, C and D, 6-bromopicolinaldehyde (0.10 g, 0.54 mmol) was converted to compound **45** (0.15 g, 0.36 mmol, 67%), a yellow solid (mp 178-180 °C decomp); t_R-HPLC: 20.1 min (97%); ^{1}H NMR (500 MHz, DMSO-d6) δ 10.17 (s, 1H), 8.15 (s, 1H), 7.92 (d, *J* = 7.7 Hz, 1H), 7.82 (t, *J* = 7.7 Hz, 1H), 7.69 (d, *J* = 7.7 Hz, 1H), 7.43 (d, *J* = 8.0 Hz, 2H), 7.07 (d, *J* = 8.0 Hz, 2H), 4.16 (s, 2H), 2.21 (s, 3H); ^{13}C NMR (125 MHz, DMSO-d6) δ 197.81, 165.17, 153.43, 144.75, 141.23, 140.34, 136.47, 132.28, 129.11, 119.53, 119.09, 38.85, 20.42; FTIR υ_{max} 3119, 2918, 1651, 1604, 1573, 1538, 1511, 1434, 1407, 1386, 1346, 1314, 1279, 1238, 1159, 1127, 1037, 985, 941, 893, 812, 798, 728, 718, 687, 650, 614 cm^{-1}; ESI-MS (m/z) calcd for $C_{16}H_{16}BrN_4OS_2$ $[M+H]^+$ 422.9949, found: 422.9951.

8.31. 2-((4-(*tert*-Butyl)phenyl)amino)-2-oxoethyl (*E*)-2-((6-bromopyridin-2-yl)methylene)hydrazine-1-carbodithioate (46)

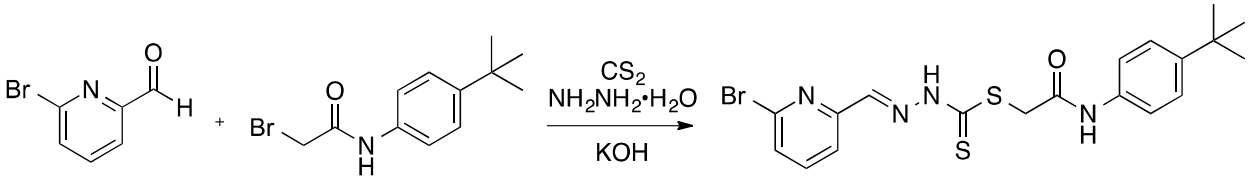

S17 **S23** **46**

Following the sequence of Procedure B, C and D, 6-bromopicolinaldehyde (0.10 g, 0.54 mmol) was converted to compound **46** (0.17 g, 0.36 mmol, 67%), a yellow solid (mp 178-180 °C

decomp); t_R-HPLC: 20.2 min (98%); ^{1}H NMR (500 MHz, DMSO-d6) δ 10.23 (s, 1H), 8.19 (s, 1H), 7.96 (d, *J* = 7.7 Hz, 1H), 7.86 (t, *J* = 7.8 Hz, 1H), 7.73 (d, *J* = 7.7 Hz, 1H), 7.50 (d, *J* = 8.7 Hz, 2H), 7.32 (d, *J* = 8.7 Hz, 2H), 4.19 (s, 2H), 1.26 (s, 9H); ^{13}C NMR (100 MHz, DMSO-d6) δ 197.85, 165.23, 153.47, 145.70, 144.78, 141.28, 140.40, 136.45, 129.18, 125.38, 119.55, 118.88, 38.88, 34.03, 31.20; FTIR υ_{max} 3225, 3176, 3114, 3049, 2953, 2905, 2869, 1646, 1593, 1531, 1430, 1339, 1324, 1302, 1272, 1243, 1156, 1145, 1110, 1036, 985, 941, 888, 831, 800, 716, 647, 610 cm^{-1}; ESI-MS (m/z) calcd for $C_{19}H_{22}BrN_4OS_2$ $[M+H]^+$ 465.0418, found: 465.0410.

8.32. 2-((4-Methoxyphenyl)amino)-2-oxoethyl (*E*)-2-((5-bromopyridin-2-yl)methylene)hydrazine-1-carbodithioate (47)

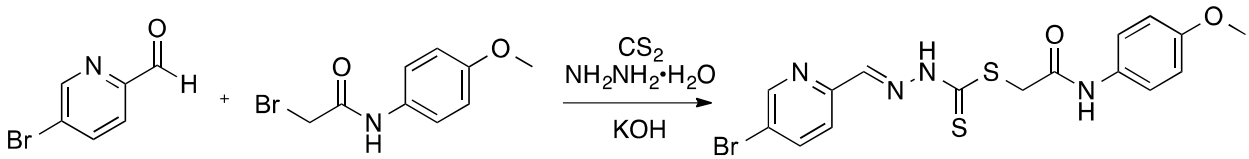

S16 **S24** **47**

Following the sequence of Procedure B, C and D, 5-bromopicolinaldehyde (0.15 g, 0.81 mmol) was converted to compound **47** (0.24 g, 0.55 mmol, 68%), a yellow solid (mp 178-180 °C decomp); t_R-HPLC: 19.8 min (99%); ^{1}H NMR (500 MHz, DMSO-d6) δ 10.16 (s, 1H), 8.78 (s, 1H), 8.25 (s, 1H), 8.17 (d, *J* = 8.4 Hz, 1H), 7.90 (d, *J* = 8.4 Hz, 1H), 7.50 (d, *J* = 8.6 Hz, 2H), 6.88 (d, *J* = 8.6 Hz, 2H), 4.18 (s, 2H), 3.72 (s, 3H); ^{13}C NMR (125 MHz, DMSO-d6) δ 197.61, 164.92, 155.27, 151.02, 150.60, 145.50, 139.82, 132.12, 121.65, 121.47, 120.62, 113.86, 55.14, 38.77; FTIR □$_{max}$ 3278, 3113, 2949, 2899, 1652, 1525, 1512, 1463, 1372, 1310, 1279, 1259, 1248, 1167, 1127, 1108, 1090, 10052, 1029, 1011, 971, 927, 876, 826, 735, 713, 644, 606, 570 cm^{-1};ESI-MS (m/z) calcd for $C_{16}H_{16}N_4O_2S_2Br$ $[M+H]^+$ 438.9898, found: 438.9889.

8.33. 2-Oxo-2-(*p*-tolylamino)ethyl (*E*)-2-(pyridin-3-ylmethylene)hydrazine-1-carbodithioate (48)

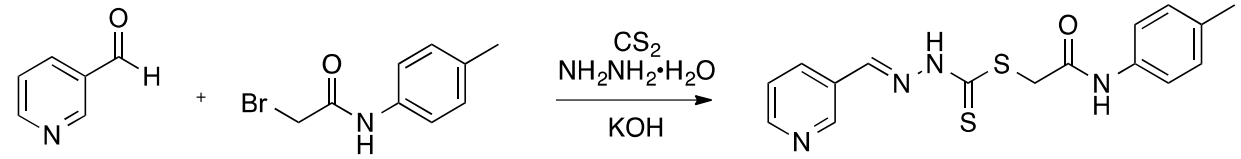

S8 **S22** **48**

Following the sequence of Procedure B, C and D, nicotinaldehyde (0.15 g, 1.40 mmol) was converted to compound **48** (0.31 g, 0.91 mmol, 65%), a yellow solid (mp 178-180 °C decomp); t_R-HPLC: 20.0 min (97%); ^{1}H NMR (400 MHz, DMSO-d6) δ 10.19 (s, 1H), 8.88 (s, 1H), 8.67 –

8.63 (m, 1H), 8.31 (s, 1H), 8.15 (d, *J* = 8.0 Hz, 1H), 7.51 (dd, *J* = 8.0, 4.7 Hz, 1H), 7.47 (d, *J* = 8.3 Hz, 2H), 7.11 (d, *J* = 8.3 Hz, 2H), 4.19 (s, 2H), 2.25 (s, 3H); ^{13}C NMR (100 MHz, DMSO-d6) δ 197.02, 165.30, 151.30, 149.08, 143.96, 136.49, 133.77, 132.23, 129.34, 129.09, 124.14, 119.08, 38.72, 20.41; FTIR υ_{max} 3247, 3116, 3033, 2918, 2853, 1657, 1593, 1521, 1484, 1415, 1370, 1333, 1304, 1246, 1191, 1162, 1104, 1033, 968, 935, 813, 750, 701, 689, 630, 606, 561 cm^{-1}; ESI-MS (m/z) calcd for $C_{16}H_{17}N_4OS_2$ $[M+H]^+$ 345.0844, found: 345.0841.

8.34. 2-((4-(*tert*-Butyl)phenyl)amino)-2-oxoethyl (*E*)-2-(pyridin-3-ylmethylene)hydrazine-1-carbodithioate (49)

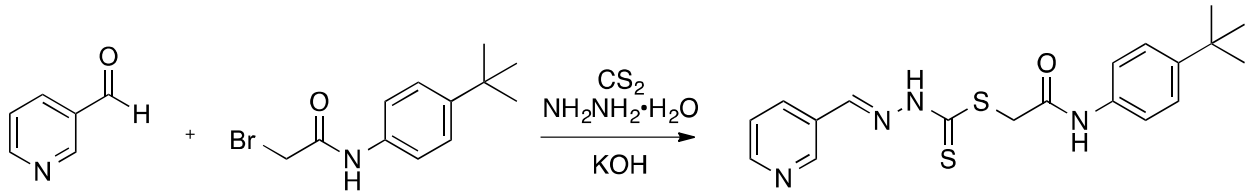

S8 **S23** **49**

Following the sequence of Procedure B, C and D, nicotinaldehyde (0.10 g, 0.93 mmol) was converted to compound **49** (0.24 g, 0.62 mmol, 66%), a yellow solid (mp 178-180 °C decomp); t_R-HPLC: 20.2 min (97%); ^{1}H NMR (500 MHz, DMSO-d6) δ 10.22 (s, 1H), 8.90 (d, *J* = 1.3 Hz, 1H), 8.67 (dd, *J* = 1.3, 4.8 Hz, 1H), 8.31 (s, 1H), 8.19 (d, *J* = 7.9 Hz, 1H), 7.54 (dd, *J* = 4.8, 7.9 Hz, 1H), 7.50 (d, *J* = 8.6 Hz, 2H), 7.32 (d, *J* = 8.6 Hz, 2H), 4.19 (s, 2H), 1.25 (s, 9H); ^{13}C NMR (125 MHz, DMSO-d6) δ 197.16, 165.40, 150.83, 148.66, 145.72, 143.78, 136.46, 134.33, 129.61, 125.37, 124.39, 118.92, 38.73, 34.03, 31.21; FTIR υ_{max} 3274, 3196, 3116, 2960, 2865, 1749, 1733, 1699, 1683, 1669, 1653, 1635, 1606, 1558, 1533, 1507, 1417, 1362, 1312, 1269, 1196, 1102, 1027, 962, 878, 833, 699, 631, 607 cm^{-1}; ESI-MS (m/z) calcd for $C_{19}H_{23}N_4OS_2$ $[M+H]^+$ 387.1313, found: 387.1313.

8.35. 2-((4-(*tert*-Butyl)phenyl)amino)-2-oxoethyl (*E*)-2-(pyridin-3-ylmethylene)hydrazine-1-carbodithioate (50)

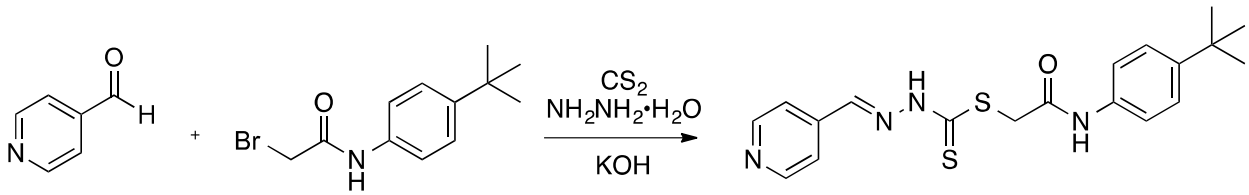

S9 **S23** **50**

Following the sequence of Procedure B, C and D, isonicotinaldehyde (0.10 g, 0.93 mmol) was converted to compound **50** (0.23 g, 0.60 mmol, 64%), a yellow solid (mp 178-180 °C decomp); t_R-HPLC: 20.3 min (98%); ^{1}H NMR (500 MHz, DMSO-d6) δ 10.23 (s, 1H), 8.68 (d, *J* = 6.0 Hz, 2H), 8.24 (s, 1H), 7.68 (d, *J* = 6.0 Hz, 2H), 7.50 (d, *J* = 8.6 Hz, 2H), 7.32 (d, *J* = 8.6 Hz, 2H), 4.19 (s, 2H), 1.26 (s, 9H); ^{13}C NMR (125 MHz, DMSO-d6) δ 197.87, 165.26, 150.43, 145.68, 144.06, 140.50, 136.43, 125.35, 121.15, 118.87, 38.76, 34.00, 31.17; FTIR υ_{max} 3273, 3185, 3115, 3031, 2956, 2863, 2743, 1683, 1669, 1653, 1601, 1540, 1471, 1362, 1328, 1268, 1233, 1205, 1119, 1056, 1000, 908, 828, 807, 732, 673, 611, 556 cm^{-1}; ESI-MS (m/z) calcd for $C_{19}H_{23}N_4OS_2$ $[M+H]^+$ 387.1313, found: 387.1313.

8.36. 2-((4-(*tert*-Butyl)phenyl)amino)-2-oxoethyl (*E*)-2-(pyrazin-2-ylmethylene)hydrazine-1-carbodithioate (51)

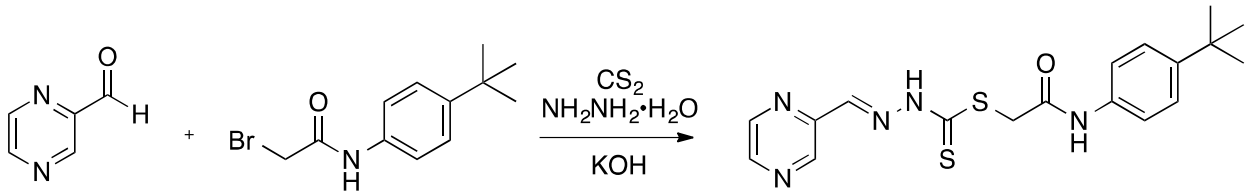

S10 **S23** **51**

Following the sequence of Procedure B, C and D, pyrazine-2-carbaldehyde (0.10 g, 0.92 mmol) was converted to compound **51** (0.23 g, 0.59 mmol, 64%), a yellow solid (mp 178-180 °C decomp); t_R-HPLC: 19.6 min (98%); ^{1}H NMR (400 MHz, DMSO-d6) δ 10.24 (s, 1H), 9.12 (d, *J* = 1.4 Hz, 1H), 8.73 – 8.68 (m, 2H), 8.31 (s, 1H), 7.50 (d, *J* = 8.7 Hz, 2H), 7.32 (d, *J* = 8.7 Hz, 2H), 4.21 (s, 2H), 1.25 (s, 9H); ^{13}C NMR (100 MHz, DMSO-d6) δ 198.09, 165.23, 147.85, 145.69, 145.25, 144.73, 144.29, 142.11, 136.45, 125.37, 118.89, 38.78, 34.02, 31.20; FTIR υ_{max} 3245, 3107, 2959, 2867, 1683, 1600, 1532, 1498, 1410, 1305, 1286, 1172, 1065, 1046, 1014,

913, 905, 874, 837, 746, 704, 612, 555 cm^{-1}; ESI-MS (m/z) calcd for $C_{18}H_{22}N_5OS_2$ $[M+H]^+$ 388.1266, found: 388.1263.

8.37. 2-Oxo-2-(*p*-tolylamino)ethyl (*E*)-2-((4-chloro-1-methyl-1*H*-pyrazol-3-yl)methylene)hydrazine-1-carbodithioate (62)

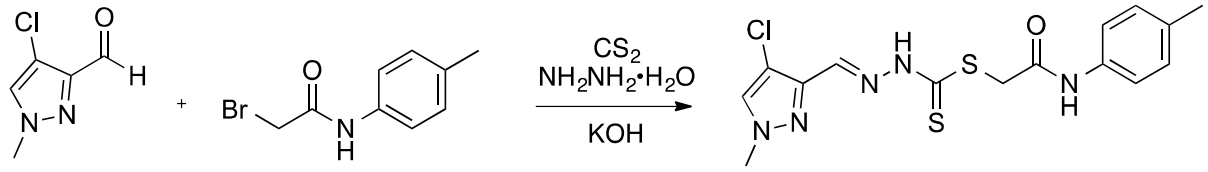

S13 **S22** **52**

Following the sequence of Procedure B, C and D, 4-chloro-1-methyl-1*H*-pyrazole-3-carbaldehyde (0.10 g, 0.69 mmol) was converted to compound **62** (0.17 g, 0.45 mmol, 65%), a yellow solid (mp 178-180 °C decomp); t_R-HPLC: 19.7 min (96%); ^{1}H NMR (400 MHz, DMSO-d6) δ 10.18 (s, 1H), 8.25 (s, 1H), 8.09 (s, 1H), 7.46 (d, *J* = 8.4 Hz, 2H), 7.10 (d, *J* = 8.4 Hz, 2H), 4.15 (s, 2H), 3.87 (s, 3H), 2.24 (s, 3H); ^{13}C NMR (100 MHz, DMSO-d6) δ 196.79, 165.48, 141.07, 139.37, 136.57, 132.22, 131.51, 129.14, 119.07, 107.87, 39.72, 38.71, 20.46; FTIR υ_{max} 3279, 3172, 3120, 3101, 3033, 2919, 2848, 1659, 1596, 1525, 1489, 1403, 1376, 1356, 1324, 1302, 1279, 1245, 1171, 1101, 1085, 1047, 1020, 963, 932, 854, 811, 726, 707, 681, 616, 572 cm^{-1}; ESI-MS (m/z) calcd for $C_{15}H_{17}N_5OS_2Cl$ $[M+H]^+$ 382.0563, found: 382.0558.

8.38. 2-((4-(*tert*-Butyl)phenyl)amino)-2-oxoethyl (*E*)-2-((4-chloro-1-methyl-1*H*-pyrazol-3-yl)methylene)hydrazine-1-carbodithioate (53)

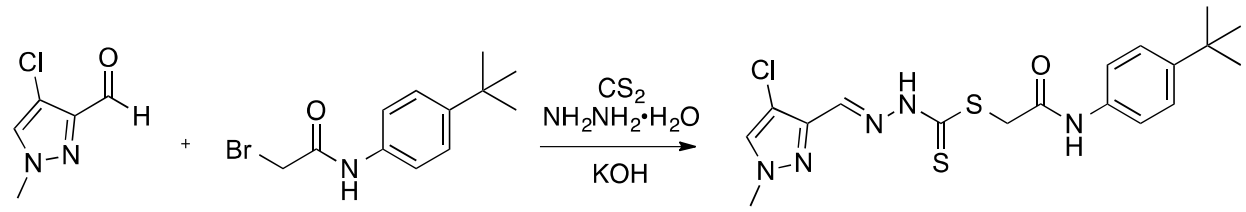

S13 **S23** **53**

Following the sequence of Procedure B, C and D, 4-chloro-1-methyl-1*H*-pyrazole-3-carbaldehyde (0.10 g, 0.69 mmol) was converted to compound **53** (0.19 g, 0.44 mmol, 64%), a yellow solid (mp 178-180 °C decomp); t_R-HPLC: 19.9 min (99%); ^{1}H NMR (500 MHz, $CDCl_3$) δ 8.67 (s, 1H), 7.44 (s, 1H), 7.40 (d, *J* = 8.4 Hz, 2H), 7.35 (s, 1H), 7.28 (d, *J* = 8.4 Hz, 2H), 4.18 (s, 2H), 3.97 (s, 3H), 1.25 (s, 9H); ^{13}C NMR (125 MHz, $CDCl_3$) δ 199.84, 166.80, 147.48, 141.45, 135.37, 129.47, 129.26, 125.88, 119.96, 112.47, 40.71, 38.06, 34.51, 31.51; FTIR υ_{max} 3277, 3119, 2959, 2866, 1661, 1600, 1515, 1489, 1442, 1404, 1361, 1321, 1279, 1191, 1155,

1100, 1084, 1020, 963, 855, 828, 727, 707, 663, 614 cm^{-1}; ESI-MS (m/z) calcd for $C_{18}H_{23}N_5OS_2Cl$ $[M+H]^+$ 424.1033, found: 424.1022.

8.39. 2-((4-Methoxyphenyl)amino)-2-oxoethyl (*E*)-2-((4-chloro-1-methyl-1*H*-pyrazol-3-yl)methylene)hydrazine-1-carbodithioate (54)

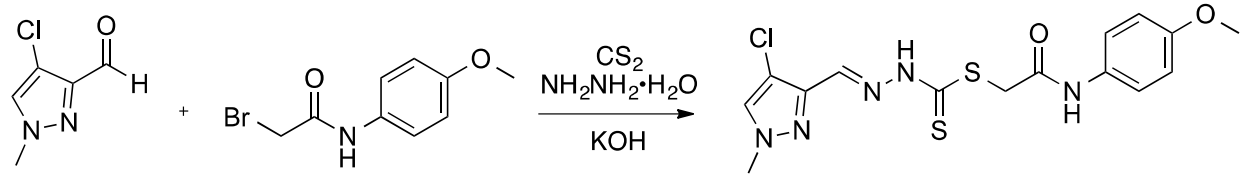

S13 **S24** **54**

Following the sequence of Procedure B, C and D, 4-chloro-1-methyl-1*H*-pyrazole-3-carbaldehyde (0.10 g, 0.69 mmol) was converted to compound **54** (0.18 g, 0.46 mmol, 67%), a yellow solid (mp 178-180 °C decomp); t_R-HPLC: 19.5 min (92%); ^{1}H NMR (500 MHz, DMSO-d6) δ 10.12 (s, 1H), 8.25 (s, 1H), 8.07 (s, 1H), 7.53 – 7.46 (m, 2H), 6.91 – 6.84 (m, 2H), 4.16 (s, 2H), 3.88 (s, 3H), 3.72 (s, 3H); ^{13}C NMR (100 MHz, DMSO-d6) δ 196.80, 165.22, 155.26, 141.08, 139.35, 132.20, 131.53, 120.64, 113.85, 107.91, 55.14, 39.72, 38.66; FTIR υ_{max} 3289, 3141, 3107, 2962, 2841, 1668, 1532, 1511, 1494, 1411, 1376, 1356, 1335, 1284, 1237, 1181, 1169, 1103, 1083, 1021, 964, 855, 822, 798, 728, 710, 686, 615, 571 $cm^{-}1$; ESI-MS (m/z) calcd for $C_{15}H_{17}N_5O_2S_2Cl$ $[M+H]^+$ 398.0512, found: 398.0505.

8.40. 2-((4-Methoxyphenyl)amino)-2-oxoethyl (*E*)-2-(thiazol-4-ylmethylene)hydrazine-1-carbodithioate (55)

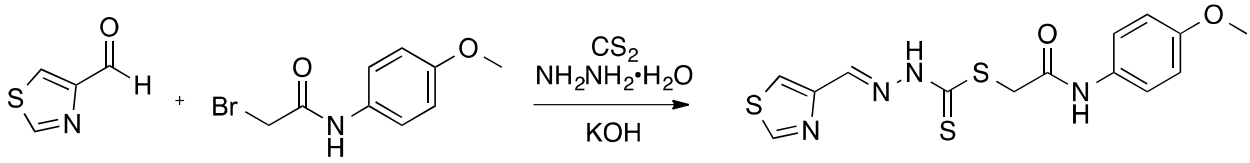

S11 **S24** **55**

Following the sequence of Procedure B, C and D, thiazole-4-carbaldehyde (0.15 g, 1.32 mmol) was converted to compound **55** (0.32 g, 0.89 mmol, 67%), a yellow solid (mp 178-180 °C decomp); t_R-HPLC: 19.8 min (98%); ^{1}H NMR (500 MHz, DMSO-d6) δ 10.13 (s, 1H), 9.21 (s, 1H), 8.41 (s, 1H), 8.24 (s, 1H), 7.49 (d, *J* = 8.6 Hz, 2H), 6.85 (d, *J* = 8.6 Hz, 2H), 4.15 (s, 2H), 3.72 (s, 3H); ^{13}C NMR (125 MHz, DMSO-d6) δ 196.60, 165.08, 155.66, 155.25, 150.43, 141.25, 132.15, 121.86, 120.62, 113.85, 55.13, 38.73; FTIR υ_{max} 3290, 3120, 3080, 2957, 2837, 2360, 2160, 1668, 1599, 1525, 1510, 1457, 1406, 1358, 1318, 1288, 1229, 1168, 1151, 1098, 1033,

966, 929, 882, 866, 827, 756, 704, 635, 572 cm^{-1}; ESI-MS (m/z) calcd for $C_{14}H_{15}N_4O_2S_3$ $[M+H]^+$ 367.0357, found: 367.0354.

9. REFERENCES

1. Sun, Q.; Collins, R.; Huang, S.; Holmberg-Schiavone, L.; Anand, G. S.; Tan, C. H.; van-den-Berg, S.; Deng, L.W.; Moore, P.K.; Karlberg, T.; Sivaraman, J. Structural Basis for the Inhibition Mechanism of Human Cystathionine Gamma-Lyase, an Enzyme Responsible for the Production of H_2S. *J. Biol. Chem.* **2009**, *284*, 3076-3085.
2. Janosik, M.; Meier, M.; Kery, V.; Oliveriusova, J.; Burkhard, P.; Kraus, J. P. Crystallization and Preliminary X-ray Diffraction Analysis of the Active Core of Human Recombinant Cystathionine Beta-Synthase: An Enzyme Involved in Vascular Disease. *Acta Crystallogr. D Biol. Crystallogr.* **2001**, *57*, 289-291.
3. Zhang, J. H.; Chung, T. D.; Oldenburg, K. R. A Simple Statistical Parameter for Use in Evaluation and Validation of High Throughput Screening Assays. *J. Biomol. Screen.* **1999**, *4*, 67-73.
4. Thorson, M. K.; Majtan, T.; Kraus, J. P.; Barrios, A. M. Identification of Cystathionine -Synthase Inhibitors Using a Hydrogen Sulfide Selective Probe. *Angew. Chem. Int. Edit.* **2013**, *52*, 4641-4644.
5. Molecular Operating Environment (MOE), 2016.0802; Chemical Computing Group Inc., 1010 Sherbooke St. West, Suite #910, Montreal, QC, Canada, H3A 2R7, 2017.
6. D.A. Case, T. A. D., T.E. Cheatham, III, C.L. Simmerling, J. Wang, R.E. Duke, R. Luo, R.C. Walker, W. Zhang, K.M. Merz, B. Roberts, S. Hayik, A. Roitberg, G. Seabra, J. Swails, A.W. Goetz, I. Kolossváry, K.F. Wong, F. Paesani, J. Vanicek, R.M. Wolf, J. Liu, X. Wu, S.R. Brozell, T. Steinbrecher, H. Gohlke, Q. Cai, X. Ye, J. Wang, M.-J. Hsieh, G. Cui, D.R. Roe, D.H. Mathews, M.G. Seetin, R. Salomon-Ferrer, C. Sagui, V. Babin, T. Luchko, S. Gusarov, A. Kovalenko, and P.A. Kollman *AMBER 12*, University of California, San Francisco, 2012.
7. Gerber, P. R.; Muller, K. Mab, A Generally Applicable Molecular-Force Field for Structure Modeling in Medicinal Chemistry. *J. Comput. Aid. Mol. Des.* **1995**, *9*, 251-268.